Functional Magnetic Resonance Imaging Versus Kidney Biopsy to Assess Response to Therapy in Nephrotic Syndrome: A Case Report

Anna Caroli, Andrea Remuzzi, Barbara Ruggiero, Camillo Carrara, Paola Rizzo, Paolo Brambilla, Piero Ruggenenti, and Giuseppe Remuzzi

In recent years, kidney functional magnetic resonance imaging (MRI) has seen great advances, with several cross-sectional studies demonstrating correlations between MRI biomarkers and glomerular filtration rate. However, the potential of MRI to monitor response to therapy in kidney disease remains undescribed. In this case report, a man in his 40s with drug-resistant membranous nephropathy was addressed to ofatumumab therapy. He underwent kidney biopsy before and 2 years after treatment and repeat non–contrast-enhanced MRI of the kidney every 6 months. An age- and sex-matched healthy volunteer was included as a normal control. The patient showed a striking positive immunologic response to therapy. Repeat MRI of the kidney documented progressive kidney functional recovery, with a significant widespread increase in kidney diffusivity, assessed using diffusion-weighted imaging, paralleling the increase in glomerular filtration rate and regression of albuminuria. Renal blood flow and ultrafiltration coefficient, assessed using phase-contrast MRI, significantly increased, suggesting an increase in filtration fraction. This case report provides the first clinical evidence in support of MRI of the kidney as a tool to noninvasively monitor pathophysiologic changes occurring in response to treatment. Although kidney biopsy remains critical for diagnosis, functional MRI of the kidney has promise for monitoring disease progression and response to therapy.

Complete author and article information provided before references.

Kidney Med. 2(6):804-809. Published online October 23, 2020.

doi: 10.1016/j.xkme.2020.07.008

INTRODUCTION

Functional magnetic resonance imaging (MRI) of the kidney has seen great advances, now offering quantitative biomarkers with the potential to improve the management of kidney disease alongside drug development.[1,2] Despite several cross-sectional studies showing the correlation between MRI biomarkers, glomerular filtration rate, and pathologic lesions,[3-7] the potential of kidney MRI to monitor response to therapy in chronic kidney disease (CKD) remains undescribed. Membranous nephropathy is a glomerular disease that is the leading cause of nephrotic syndrome in nondiabetic White adults.[8,9] In patients with membranous nephropathy with drug-resistant nephrotic syndrome, fully humanized anti-CD20 antibodies show promise as a possible therapeutic option.[10-12]

The aim of this study was to provide first evidence of the clinical utility of MRI of the kidney as a noninvasive marker of drug-induced pathophysiologic change by documenting kidney microstructural and functional recovery occurring in a patient with drug-resistant membranous nephropathy who was administered ofatumumab.

CASE REPORT

A man in his 40s with primary membranous nephropathy received a 6-month course of steroid and chlorambucil treatment at disease onset. This was ineffective, but 1 year later a 2-year course of oral cyclosporine achieved partial remission of nephrotic syndrome (proteinuria with protein excretion < 1 g/d) until the patient experienced a relapse 6 years later. Cyclosporine treatment was reintroduced for 1 year but kidney function started worsening and a control biopsy revealed significant glomerulosclerosis associated with stripped interstitial fibrosis with tubular lesions, indicating calcineurin inhibitor toxicity. Five years later, a single 375-mg/m^2 dose of rituximab failed to achieve remission. The following year, the patient was admitted to the Bergamo hospital and prescribed ofatumumab therapy, receiving 1 single 300-mg infusion. The patient was maintained on conservative therapy with perindopril and irbesartan, with unchanged dose except for transient irbesartan downtitration due to hypotension. A healthy volunteer from a previous study of MRI of the kidney (ClinicalTrials.gov Identifier: NCT02618460) was included in the study as an age- and sex-matched normal control.

Before ofatumumab treatment, the patient had severely decreased kidney function, notable for proteinuria and anti-phospholipase A_2 receptor (PLA_2R) antibody serum concentration (Table 1).

The patient underwent non–contrast-enhanced MRI of the kidney to noninvasively investigate pretreatment pathophysiology. As described in the supplementary methods (Item S1), pure diffusivity, pseudo-diffusion, and flowing fraction parameters were estimated using diffusion-weighted MRI (DWI). Renal blood flow and derivative parameters (renal plasma flow, filtration fraction, renal vascular resistance, and glomerular filtration coefficient [K_f]) were assessed using phase-contrast MRI. DWI scans showed areas of irregular diffusivity, suggestive of parenchymal lesions of different severity (Fig 1A). Kidney median diffusivity was much lower than normal, with an inversion of the difference between cortical and medullary values

Table 1. Clinical, Laboratory and MRI Parameters in a Patient With Membranous Nephropathy Treated With Ofatumumab and in an Age- and Sex-Matched Healthy Control Person; Histologic Characterization of the Patient Biopsy Samples, Collected Before and 2 Years After Therapy

	Patient					
	Baseline (pre-ofatumumab)	6 mo	12 mo	18 mo	24 mo	Healthy Control
Clinical and Laboratory parameters						
Systolic blood pressure, mm Hg	102	114	108	117	116	120
Diastolic blood pressure, mm Hg	65	70	66	67	78	80
Serum creatinine, mg/dL	3.16	2.08	1.76	1.72	1.34	0.82
Serum albumin, g/dL	2.2	3.2	3.5	3.8	3.8	—
Serum proteins, g/dL	4.7	5.2	6.0	6.2	6.6	7.2
Hematocrit, %	34.9	27.7	36.2	40.5	44.3	42.5
Anti-phospholipase A_2 antibodies, RU/mL	145.6	4.2	1.1	<2	<2	—
24-h proteinuria, g/d	14.2	2.9	1.5	0.86	1.3	—
GFR (CKD-EPI estimated), mL/min/1.73 m^2	20.7	35.1	42.1	43.5	59.2	110.2
GFR (iohexol-measured), mL/min/1.73 m^2	33.1	37.6	46.1	52.9	65.9	—
MRI Parameters						
Phase contrast MRI						
RBF, mL/min/1.73 m^2	608.5	—	832.9	—	852.8	913.4
RPF, mL/min/1.73 m^2	396.1	—	530.6	—	475.0	525.2
FF, %	8.25	—	8.60	—	14.05	20.18
Pgc, mm Hg, assumed	45.00	—	47.00	—	54.00	60.00
K_f, mL/min/mm Hg	2.18	—	4.46	—	5.44	8.91
RVR, dyn s/cm^5	9.16	—	6.89	—	7.77	7.90
Diffusion-weighted MRI						
D, kidney, $cm^2/s \times 10^{-3}$	1.45[a] [1.29-1.62]	—	1.56[b] [1.33-1.73]	1.58[b] [1.39-1.77]	1.63[b] [1.31-1.82]	1.79 [1.62-1.95]
D, cortex, $cm^2/s \times 10^{-3}$	1.46[a] [1.35–1.59]	—	1.60[b] [1.43-1.73]	1.69[b] [1.52-1.87]	1.68[b] [1.51-1.82]	1.84 [1.74-2.01]
D, medulla, $cm^2/s \times 10^{-3}$	1.60[a] [1.43-1.79]	—	1.56[b] [1.32-1.76]	1.61 [1.35-1.84]	1.66[b] [1.41-1.85]	1.77 [1.60-1.97]
ΔD_{C-M}, $cm^2/s \times 10^{-3}$	−0.142	—	0.040	0.077	0.016	0.065
D*, kidney, $cm^2/s \times 10^{-3}$	2.53[a] [2.21-3.04]	—	2.38[b] [1.95-3.11]	3.36[b] [2.95-3.89]	3.27[b] [2.70-4.17]	2.86 [2.49-3.35]
F, kidney [0-1]	0.25[a] [0.18-0.36]	—	0.25[b] [0.15-0.36]	0.31[b] [0.23-0.40]	0.27[b] [0.19-0.40]	0.21 [0.12-0.30]
Histologic Characterization						
Cortical peritubular interstitial volume, %	51.00 [48.43-54.15]	—	—	—	36.31[b] [33.17-39.66]	—
Fibrosis, %	10.29 [9.22-11.36]	—	—	—	9.31 [7.76-12.34]	—

Note: The 24-hour proteinuria is mean of 3 consecutive measurements; GFR was measured using the iohexol plasma clearance (patient) or estimated using the CKD-EPI formula (control). Diffusion-weighted MRI parameters, peritubular interstitial volume, and fibrosis are expressed as median [interquartile range]. *P* values are computed using Wilcoxon signed rank test with Bonferroni correction.

Abbreviations ΔD_{C-M}, difference between cortical and medullary D medians; CKD-EPI, Chronic Kidney Disease Epidemiology Collaboration; D, true diffusion coefficient; D*, pseudo-diffusion coefficient (molecular motion caused by microperfusion and tubular flow); F, flowing fraction; FF, filtration fraction; GFR, glomerular filtration rate; K_f, glomerular ultrafiltration coefficient; MRI, magnetic resonance imaging; Pgc, glomerular capillary pressure; RBF, renal blood flow; RPF, renal plasma flow; RVR, renal vascular resistance.

[a] $P < 0.001$ versus control;

[b] $P < 0.001$ versus baseline.

(ΔD_{C-M}; Table 1; Fig 1H). Renal plasma flow, filtration fraction, and K_f were notably lower, whereas renal vascular resistance was notably higher than normal (Table 1).

The pretreatment biopsy confirmed the presence of severe chronic changes (Fig 2E-H). Light microscopy revealed 23 glomeruli, 13% and 20% of which were globally and segmentally sclerosed, respectively. Glomeruli showed diffuse thickening of peripheral capillary walls and segmental epimembranous "spikes" (Fig 2E). The tubulointerstitial compartment demonstrated patchy tubular atrophy and diffuse moderate interstitial fibrosis. Moderate acute tubular injury, discrete interstitial edema, and mild

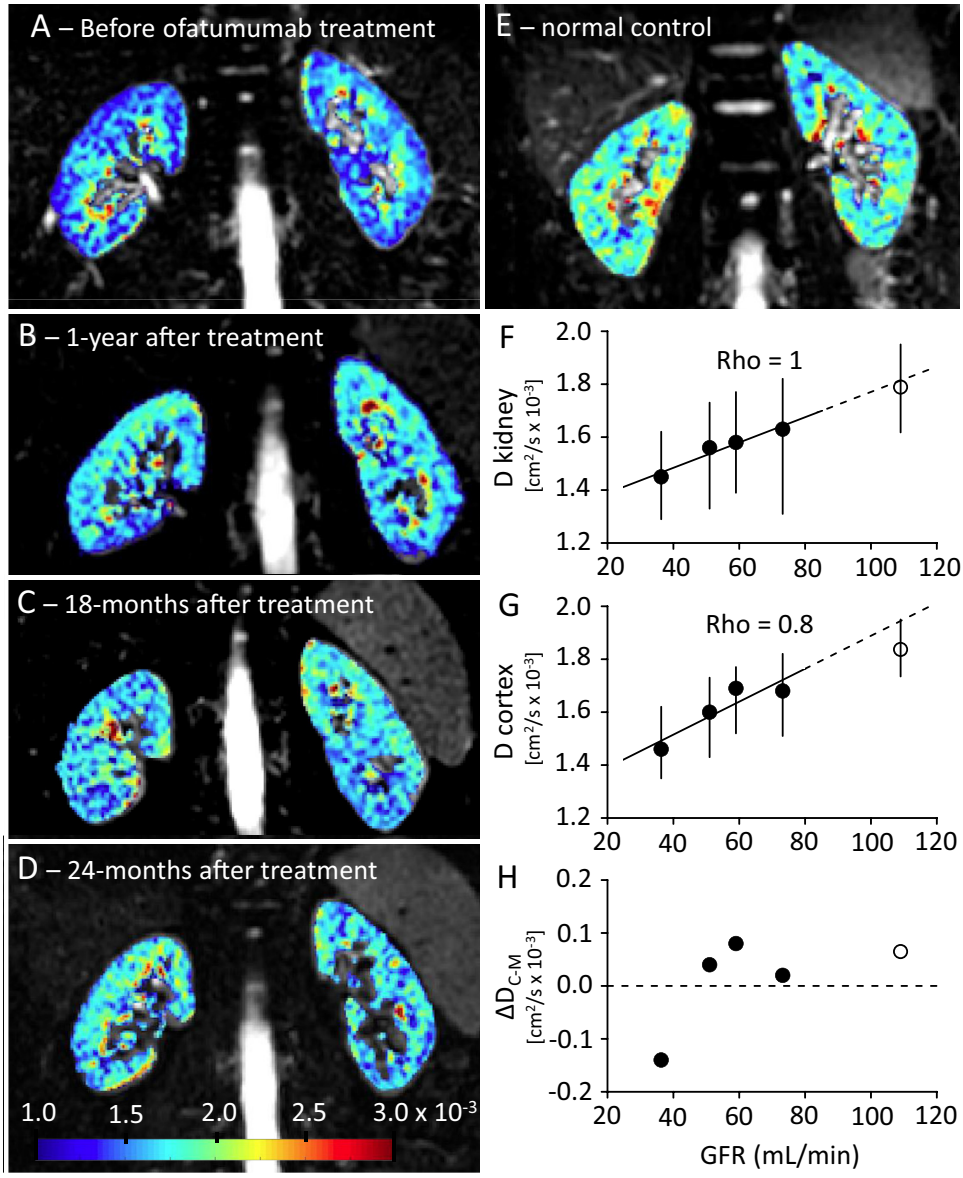

Figure 1. Kidney diffusion-weighted imaging (DWI) longitudinal findings, reflecting positive clinical response to ofatumumab therapy in a patient with membranous nephropathy. (A) Pretreatment DWI-based kidney diffusivity (D) map shows areas of irregular D, both at the intraparenchymal level and across the patient kidneys. (B) One-year posttreatment D map shows significant widespread improvement in kidney D, especially in the cortex. (C, D) The 18- and 24-month posttreatment D maps show further improvement in kidney D. (E) Normal D in an age- and sex-matched healthy control. (F) Correlation between median kidney D (expressed in $cm^2/s \times 10^{-3}$) and glomerular filtration rate (GFR, expressed in mL/min) in the patient over time as compared with the normal control. (G) Correlation between cortical D and GFR in the patient over time as compared with the normal control. (H) Difference between cortical and medullary D (ΔD_{C-M}), going back to normal positive values after treatment. Black dots represent the patient over time, white dots represent normal control values. Rho denotes Spearman rank correlation coefficient.

inflammatory infiltrates were found. The arteries showed moderate arteriosclerosis. Immunofluorescence studies showed granular peripheral capillary wall staining for immunoglobulin G (IgG; 3+) and κ (2+) and λ light chains (3+; Fig 2F). There was no significant staining for IgA, IgM, C3, C1q, or fibrinogen. Electron microscopy demonstrated diffuse subepithelial and intramembranous electron-dense deposits, with severe podocyte foot-process effacement (Fig 2H).

The patient showed a striking positive immunologic response to ofatumumab therapy, with complete circulating B-cell depletion within 24 hours and anti-PLA_2R autoantibody depletion within 6 months (Fig 2A; Table 1). At 6 months after treatment, nephrotic syndrome was in remission. Measured glomerular filtration rate (GFR) increased over time (Fig 2C; Table 1); the last proteinuria approximated a complete clinical remission (Fig 2B; Table 1).

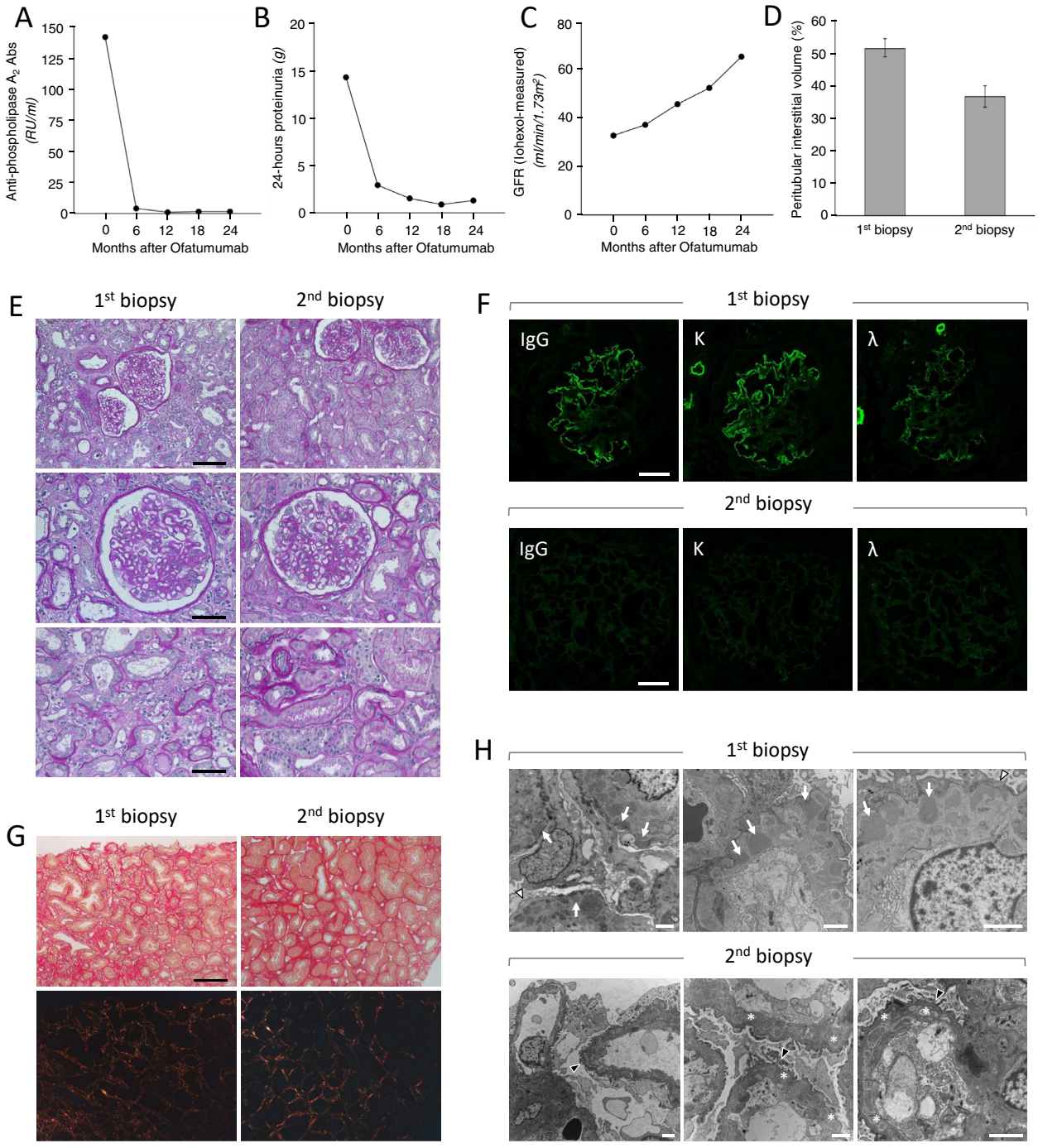

Figure 2. Clinical and histologic response to ofatumumab therapy in a patient with membranous nephropathy. (A) Positive immunologic response, (B) decrease in proteinuria, (C) progressive glomerular filtration rate (GFR) increase, and (D) cortical peritubular interstitial volume reduction occurring after therapy. (E) Representative microscopy images stained with periodic acid–Schiff demonstrate severe chronic changes appearing before (1st biopsy, left) and 2 years after treatment (2nd biopsy, right), and acute tubular injury, interstitial edema, and inflammation, significantly decreasing after treatment. Scale bars, 50 μm (top row) and 20 μm (middle and bottom rows). (F) Representative immunofluorescence microscopy images show complete disappearance of the typical glomerular immunoglobulin G (IgG) staining and significant weakening of κ and λ light chain staining after therapy. Scale bar, 50 μm. (G) Representative images of Serius red–stained sections at light microscopy (top) or polarized light (bottom), showing comparable degree of interstitial fibrosis between the pre- and 2-year posttreatment biopsies. Scale bar, 50 μm. (H) Representative transmission electron micrographs of glomerular ultrastructure show diffuse subepithelial and intramembranous electron-dense deposits (white arrows) with severe podocyte foot-process effacement (white arrowheads) before therapy, and almost complete reabsorption of subepithelial electron-dense deposits (asterisks), with a partial recovery of podocyte foot processes (black arrowheads) 2 years after therapy. Scale bars, 2,000 nm. Abbreviation: Ab, antibody.

Follow-up MRI of the kidney confirmed the positive clinical response to therapy and showed progressive kidney microstructural and functional recovery. After 1 year, whole kidney and cortical diffusivity showed a significant widespread improvement ($P < 0.001$; Fig 1B), and ΔD_{C-M} went back to positive (Table 1), suggesting a significant microstructural recovery. After 18 and 24 months, diffusivity further improved (Fig 1C and D; Table 1), paralleling the increase in GFR (Spearman $\rho = 1$ and 0.8, respectively; Fig 1F and G) and albumin levels ($\rho = 0.949$ in both cases), and ΔD_{C-M} remained positive (Fig 1H). Renal blood flow and renal plasma flow significantly increased, reaching normal values at 12 months, whereas filtration fraction and K_f significantly improved but remained lower than normal (Table 1). Renal vascular resistance significantly decreased, reaching the control value at 24 months.

To investigate the mechanisms responsible for the positive clinical response and kidney function recovery shown by MRI, the patient underwent a follow-up biopsy 2 years after therapy after signing a dedicated informed consent form. The posttreatment kidney biopsy revealed 29 glomeruli, 30% and 24% of which were globally and segmentally sclerosed, respectively. Glomeruli showed diffuse thickening of peripheral capillary walls and mild expansion of the mesangial regions. The arteries were moderately thickened. Tubular atrophy and interstitial fibrosis remained stable (Fig 2E and G; Table 1), while acute tubular injury, edema, and inflammation significantly decreased. The cortical peritubular interstitial volume significantly decreased (Fig 2D; Table 1). Immunofluorescence studies showed complete disappearance of glomerular IgG staining, alongside weak segmental glomerular staining for κ and λ light chains (Fig 2F). Electron microscopy demonstrated entirely reabsorbed intramembranous immune deposits, with partial recovery of podocyte foot processes (Fig 2H).

DISCUSSION

This study provides the first evidence of the clinical utility of functional MRI of the kidney to monitor response to therapy in kidney disease. Functional MRI markers, offering the unique opportunity to noninvasively assess pathologic changes in vivo on a whole-organ basis, correlated with clinical outcomes, including both proteinuria and kidney function, overcoming the inherent limitations of kidney biopsy.

MRI of the kidney monitoring potential has been already demonstrated in patients with autosomal dominant polycystic kidney disease[13,14] and with renal angiomyolipomas in a tuberous sclerosis complex treated with everolimus.[15] In CKD, despite large evidence of correlation between DWI-based parameters, GFR, and pathologic lesions,[3] there is only 1 longitudinal study showing the potential for kidney DWI to evaluate therapeutic efficacy, in lupus nephritis.[16] In patients with other chronic nephropathies, proteinuria, alongside GFR, is still considered the most reliable biomarker to assess response to treatment and prognosis.[17] However, early kidney damage and remission of kidney lesions may be difficult to evaluate by proteinuria due to the prolonged time required to form sufficient deposits to cause proteinuria and the time required to clear subepithelial deposits, repair podocyte and capillary wall damage, and restore glomerular permselectivity causing residual proteinuria.[9,18]

Kidney biopsy provides relevant information on kidney microstructure and shows prognostic potential.[19,20] However, it is invasive, susceptible to sampling bias, feasible only in a proportion of patients with CKD, and difficult to perform repeatedly to assess serial changes. For these reasons it is generally performed only once, in routine clinical practice, for diagnostic purposes.

MRI of the kidney, with no need for intravenous contrast agents or ionizing radiations, is well suited to serial application and could provide relevant pathophysiologic information from the earliest disease stage, also enabling assessment of functional heterogeneity across the kidney and detection of corticomedullary and left-right differences.

The main treatment effect, aside from the positive immunologic response, was the recovery of filtration function, documented by a notable increase in K_f and glomerular permselectivity toward circulation proteins, likely due to amelioration of the glomerular membrane ultrastructure. This was associated with substantial recovery of tubular injury and reduction of interstitial volume, suggesting partial remission of tubular function associated with reduced loss of filtered albumin, explaining the improvement of tubular and interstitial changes.

The increase in diffusivity assessed using DWI after therapy was associated with improved glomerular filtration, reduction of interstitial volume, and amelioration of tubular structure and function. Although an inversion in ΔD_{C-M} was previously associated with cortical interstitial fibrosis,[21,22] our study suggests its possible association with tubular fluid decrease and interstitial volume expansion. Increased tubulointerstitial space, likely indicative of fibro-edema resulting from the inflammatory response to proteinuria, could be the main cause of reduced diffusivity detected before therapy, whereas the progressive increase in diffusivity after therapy could result from interstitial volume reduction. Cortical peritubular interstitial volume, rather than fibrosis, which is a chronic kidney damage unlikely to be reversible, could represent a possible therapeutic target for membranous nephropathy.

Limitations include the lack of follow-up MRI for the control volunteer, which prevented us from showing the stability of MRI measurements in stable clinical conditions, and the lack of medullary tissue in the biopsy samples, which prevented investigation of possible changes occurring in the medulla.

In conclusion, despite being demonstrated in only a single case, this study provides the rational for future studies aimed at validating the potential of MRI of the

kidney to noninvasively monitor pathophysiologic changes occurring in response to CKD treatment. Despite kidney biopsy remaining unique for diagnosis, functional MRI could replace repeat biopsy for monitoring disease progression, both in long-term and acute clinical settings, and for assessing response to therapy. Future studies in patients with different kidney diseases followed up over a suitable period under controlled conditions are needed to determine whether MRI of the kidney could replace biopsy in any of these clinical settings.

SUPPLEMENTARY MATERIAL

Supplementary File (PDF)

Item S1: Supplementary Methods

ARTICLE INFORMATION

Authors' Full Names and Academic Degrees: Anna Caroli, PhD, Andrea Remuzzi, MEng, Barbara Ruggiero, MD, Camillo Carrara, MD, Paola Rizzo, PhD, Paolo Brambilla, MD, Piero Ruggenenti, MD, and Giuseppe Remuzzi, MD.

Authors' Affiliations: Istituto di Ricerche Farmacologiche Mario Negri IRCCS, Bergamo (AC, BR, CC, PRizzo, PRuggenenti, GR); Department of Management, Information and Production Engineering, University of Bergamo, Dalmine (BG) (AR); Division of Nephrology, Department of Pediatric Subspecialties, Ospedale Pediatrico Bambino Gesù - IRCCS, Rome (BR); Unit of Nephrology and Dialysis (CC, PRuggenenti) and Department of Diagnostic Radiology (PB), Azienda Socio-Sanitaria Territoriale Papa Giovanni XXIII, Bergamo; and Department of Biomedical and Clinical Sciences, University of Milan, Milan, Italy (GR).

Address for Correspondence: Anna Caroli, PhD, Istituto di Ricerche Farmacologiche Mario Negri IRCCS, Via Camozzi 3, 24020 Ranica (BG), Italy. E-mail: acaroli@marionegri.it

Support: None.

Financial Disclosure: The authors declare that they have no relevant financial interests.

Patient Consent: The local ethical committee (Comitato etico di Bergamo, Italy) waived the need for consent given the de-identified nature of the case report.

Peer Review: Received June 11, 2020. Evaluated by 3 external peer reviewers, with direct editorial input from the Editor-in-Chief. Accepted in revised form July 27, 2020.

REFERENCES

1. Caroli A, Pruijm M, Burnier M, Selby NM. Functional magnetic resonance imaging of the kidneys: where do we stand? The perspective of the European COST Action PARENCHIMA. *Nephrol Dial Transplant*. 2018;33(suppl_2):ii1-ii3.
2. Selby NM, Blankestijn PJ, Boor P, et al. Magnetic resonance imaging biomarkers for chronic kidney disease: a position paper from the European Cooperation in Science and Technology Action PARENCHIMA. *Nephrol Dial Transplant*. 2018;33(suppl_2):ii4-ii14.
3. Caroli A, Schneider M, Friedli I, et al. Diffusion-weighted magnetic resonance imaging to assess diffuse renal pathology: a systematic review and statement paper. *Nephrol Dial Transplant*. 2018;33(suppl_2):ii29-ii40.
4. Pruijm M, Mendichovszky IA, Liss P, et al. Renal blood oxygenation level-dependent magnetic resonance imaging to measure renal tissue oxygenation: a statement paper and systematic review. *Nephrol Dial Transplant*. 2018;33(suppl_2):ii22-ii28.
5. Wolf M, de Boer A, Sharma K, et al. Magnetic resonance imaging T1- and T2-mapping to assess renal structure and function: a systematic review and statement paper. *Nephrol Dial Transplant*. 2018;33(suppl_2):ii41-ii50.
6. Odudu A, Nery F, Harteveld AA, et al. Arterial spin labelling MRI to measure renal perfusion: a systematic review and statement paper. *Nephrol Dial Transplant*. 2018;33(suppl_2):ii15-ii21.
7. Villa G, Ringgaard S, Hermann I, et al. Phase-contrast magnetic resonance imaging to assess renal perfusion: a systematic review and statement paper. *MAGMA*. 2020;33(1):3-21.
8. Glassock RJ. Diagnosis and natural course of membranous nephropathy. *Semin Nephrol*. 2003;23(4):324-332.
9. Couser WG. Primary membranous nephropathy. *Clin J Am Soc Nephrol*. 2017;12(6):983-997.
10. Basu B. Ofatumumab for rituximab-resistant nephrotic syndrome. *N Engl J Med*. 2014;370(13):1268-1270.
11. Ruggenenti P, Fervenza FC, Remuzzi G. Treatment of membranous nephropathy: time for a paradigm shift. *Nat Rev Nephrol*. 2017;13(9):563-579.
12. Ruggenenti P, Remuzzi G. A first step toward a new approach to treating membranous nephropathy. *N Engl J Med*. 2019;381(1):86-88.
13. Bae KT, Grantham JJ. Imaging for the prognosis of autosomal dominant polycystic kidney disease. *Nat Rev Nephrol*. 2010;6(2):96-106.
14. Zhang W, Blumenfeld JD, Prince MR. MRI in autosomal dominant polycystic kidney disease. *J Magn Reson Imaging*. 2019;50(1):41-51.
15. Brakemeier S, Vogt L, Adams L, et al. Treatment effect of mTOR-inhibition on tissue composition of renal angiomyolipomas in tuberous sclerosis complex (TSC). *PloS One*. 2017;12(12):e0189132.
16. Li X, Xu X, Zhang Q, et al. Diffusion weighted imaging and blood oxygen level-dependent MR imaging of kidneys in patients with lupus nephritis. *J Transl Med*. 2014;12:295.
17. Ruggenenti P, Perticucci E, Cravedi P, et al. Role of remission clinics in the longitudinal treatment of CKD. *J Am Soc Nephrol*. 2008;19(6):1213-1224.
18. Francis JM, Beck LHJ, Salant DJ. Membranous nephropathy: a journey from bench to bedside. *Am J Kidney Dis*. 2016;68(1):138-147.
19. Srivastava A, Palsson R, Kaze AD, et al. The prognostic value of histopathologic lesions in native kidney biopsy specimens: results from the Boston Kidney Biopsy Cohort Study. *J Am Soc Nephrol*. 2018;29(8):2213-2224.
20. Zhang X-D, Cui Z, Zhang M-F, et al. Clinical implications of pathological features of primary membranous nephropathy. *BMC Nephrol*. 2018;19(1):215.
21. Friedli I, Crowe LA, Berchtold L, et al. New magnetic resonance imaging index for renal fibrosis assessment: a comparison between diffusion-weighted imaging and T1 mapping with histological validation. *Sci Rep*. 2016;6:30088.
22. Berchtold L, Friedli I, Crowe LA, et al. Validation of the cortico-medullary difference in magnetic resonance imaging-derived apparent diffusion coefficient for kidney fibrosis detection: a cross-sectional study. *Nephrol Dial Transplant*. 2020;35(6):937-945.